Final accepted version

Activity of pursuit-related neurons in Medial Superior Temporal area (MST) during static roll-tilt

Keishi Fujiwara[1,2], Teppei Akao[1], Sergei Kurkin[1] , Kikuro Fukushima[1]

[1]Department of Physiology, Hokkaido University School of Medicine, Sapporo 060-8638, Japan

[2]Depertment of Otolaryngology-Head and Neck Surgery, Hokkaido University School of Medicine, Sapporo 060-8638, Japan

Running head: MST neuron activity during static roll-tilt

Key Words: MST –Smooth-pursuit – Optic flow –Coordinate - Preferred direction - Resting rate – Static roll-tilt - Monkey

Text pages (including cover, abstract, references, table- and figure- legends): 26

Table: 2

Figures: 10

Correspondence to: Kikuro Fukushima
Department of physiology
Hokkaido University School of Medicine
West 7, North 15, Sapporo, 060-8638 Japan
Phone: +81 11 706- 5038
FAX: +81 11 706-5041
E mail: kikuro@med.hokudai.ac.jp

Recent studies have shown that rhesus macaques can perceive visual motion-direction in earth-centered coordinates as accurately as humans. We tested whether coordinate frames representing smooth-pursuit and/or visual motion signals in MST are earth-centered to better understand its role in coordinating smooth-pursuit eye movements. In 2 Japanese macaques, we compared preferred directions (re monkeys' head/trunk axis) of pursuit and/or visual motion responses of MSTd neurons while upright and during static whole-body roll-tilt. In the majority (41/51=80%) of neurons tested, preferred directions of pursuit and/or visual motion responses were similar while upright and during 40° static roll-tilt. Preferred directions of the remaining 20% of neurons (n=10) were shifted beyond the range expected from ocular counter-rolling; the maximum shift was 14° and the mean shift was 12°. These shifts, however, were still less than half of the expected shift if MST signals are coded in the earth-centered coordinates. Virtually all tested neurons (44/46=96%) failed to exhibit a significant difference between resting discharge rate while upright and during static roll-tilt while fixating a stationary spot. These results suggest that smooth-pursuit and/or visual motion signals of MST neurons are not coded in the earth-centered coordinates We suggest that these signals are coded in the head-centered coordinate.

Introduction

We asked whether the discharge coding smooth-pursuit eye movements and/or visual motion signals in MST is in the head-centered coordinate or earth-centered coordinate in order to better understand the role of MST in smooth-pursuit eye movements. The smooth-pursuit system has evolved in primates to maintain the image of a small object of interest on the foveae during object tracking and uses the velocity of retinal image-slip of the target to drive eye velocity to match target velocity (see Leigh and Zee 2006 for a review). MST contains all of the signals needed to reconstruct target motion in space including retinal image-slip velocity of a target and eye velocity during pursuit (Dürsteler et al. 1987; Dürsteler and Wurtz 1988; Komatsu and Wurtz 1988a,b; Newsome et al. 1988; Thier and Erickson 1992; Bremmer et al. 1997, 1999; Dicke and Thier 1999). MST neurons also have large visual receptive fields and strong directional selectivity for visual motion (Saito et al. 1986; Komatsu and Wurtz 1988a; Graziano et al. 1994) and they respond to whole-body rotation that activates semicircular canals (Kawano et al. 1984; Thier and Erickson 1992) as well as to whole-body translation that activates otolith organs (Duffy 1998; Gu et al. 2006, 2007, 2008; Chen et al. 2008).

MST is also involved in perception of visual motion (Celebrini and Newsome 1994, 1995). Electrical microstimulation of MST biases the monkeys' decision in a heading discrimination task, suggesting that MST has a primary role in perception of self-motion direction (Britten and Wezel 1998, 2002). It has been suggested that visual motion and vestibular signals are integrated in MST for perception of self-motion (Shenoy et al. 1999; Page and Duffy 2003; Gu et al. 2007, 2008; Chen et al. 2008). In particular, Gu et al. (2007, 2008) suggested that MSTd neurons are involved in perception of object motion by integrating eye and head movement-related signals (also Inaba et al. 2007; Liu and Angelaki 2009). However, dissociation of the activity of single MST neurons and a monkeys' behavioral choice has also been reported in a two-alternative, forced-choice task using optic flow information (Heuer and Britten 2004). So, whether MST is involved in the perception of visual motion is still controversial.

Spatial signals about visual object motion and/or pursuit eye velocity could be represented in a

variety of coordinate systems such as eye-centered, head-centered or earth-centered coordinates. While upright, these coordinates are mostly congruent but, during static whole-body roll-tilt, the earth-centered coordinate can be distinguished from the other two because ocular counter-rolling during static roll-tilt is minimal (gain = 0.1-0.2) in primates (Krejcova et al. 1971; Suzuki et al. 1997; see Leigh and Zee 2006 for a review).

The subjective direction of gravity under static whole-body roll-tilt is called the subjective visual vertical (SVV) and otolith inputs must contribute substantially to the SVV (Kaptein and Van Gisbergen 2004). Human subjects can align the perceived motion direction of a random-dot pattern to the direction of gravity in a laterally tilted position (De Vrijer et al. 2008). For this, retinal motion signals must be combined with head position signals in space. By measuring the SVV, Dadaoua et al. (2008) and Lewis et al. (2008) have shown that rhesus macaques can also perceive the earth-centered axis as accurately as humans. These results suggest that in the brain areas involved in perception of motion direction, coordinates representing visual motion signals should be earth-centered, not eye-centered or head-centered.

In the present study we examined the preferred directions (re monkeys' head/trunk axis) of pursuit and/or visual motion responses of MST neurons while upright and during static whole-body roll-tilt in head- and trunk-restrained monkeys. If MST is indeed involved in the perception of motion direction, it is most likely that coordinates representing these signals would be coded in the earth-centered coordinate. We also asked whether MST pursuit-related neurons could signal static whole-body roll-tilt. This signal would be needed for perception of motion direction during static roll-tilt. Some of the results have been presented in preliminary form (Fujiwara et al. 2008).

Materials and Methods

General procedures

Two Japanese monkeys (Y and S *Macaca fuscata* 5.6 and 5.0 kg) were used in this study. All procedures were performed in strict compliance with the Guide for the Care and Use of Laboratory Animals of National Institutes of Health. Our specific protocols were approved by the Animal Care

and Use Committee of Hokkaido University School of Medicine. Each monkey was sedated with ketamine hydrochloride [5 mg/kg, intramuscularly (i.m.)] or midazolam (0.3 mg/kg) and medetomidine (0.03 mg/kg) i.m., and then anesthetized with sodium pentobarbital [25 mg/kg, intraperitoneally (i.p.)]. Additional anesthesia (0.5-1.0 % halothane mixed with 50 % nitrous oxide and 50 % oxygen) was administered as necessary. Under aseptic conditions, head holders were affixed to the skull to allow stabilization during recording experiments. A scleral search coil was implanted underneath the conjunctiva of each eye to record vertical and horizontal components of eye movements for both eyes (Fuchs and Robinson 1966). A recording chamber was stereotaxically implanted (center aimed at posterior 5 mm and lateral 15 mm) on the skull to allow single-unit recording in MST (e.g., Komatsu and Wurtz 1988a,b; Newsome et al. 1988; Akao et al. 2005) (monkey Y from the right hemisphere and monkey S from the left hemisphere). Analgesics (pentazocine, 0.2 mg/kg) and antibiotics (flomoxef sodium, 50 mg/kg) were administered postsurgically.

Figure 1 near here

Recording procedures and behavioral paradigms

Each monkey was seated in a primate chair in darkness with the head restrained in the stereotaxic plane, facing a 15-inch LCD display (EIZO, FlexScan L365, frame rate 75 Hz) placed 20.5 cm away from the eyes. The display subtended 106° by 96° of the visual angle. The animal's trunk was also restrained by polystyrene foam in the primate chair (Kasahara et al. 2006). Monkeys were rewarded for pursuit eye movements or fixation of a small target spot (0.5° in diameter) while in an upright posture and during static whole-body roll-tilt. The spot and a random-dot pattern were presented on the display as visual stimuli. The random-dot pattern consisted of 40 randomly distributed squares; the size of each square ranged between 0.5 and 1.5° and the pattern covered 20 × 20° of visual angle and the orientation of these squares was randomized. The luminous intensities of the target spot, random-dots, and background were 3.1, 4.7, and 0.1 cd/m^2, respectively. The display and the primate chair together with the monkey were tilted in the roll plane to 40° from the

earth-centered (either right ear down direction, or left ear down direction, Fig. 1A, RED, LED, respectively).

For our search task, the target moved sinusoidally along oblique trajectories (0.5 Hz, ±10°) across the stationary background pattern in order to locate neurons whose activity was related to smooth-pursuit and/or visual motion. Once responsive single neurons in MST were encountered, as judged visually and on the audio monitor, neuronal responses were tested during smooth-pursuit in 8 cardinal directions separated by 45° (horizontal, vertical and oblique directions, Fig. 1A, upright) with and without the stationary background pattern. To analyze preferred directions during smooth-pursuit, the target moved at 20°/sec in a ramp trajectory from -10° to +10° in each direction. The target stayed stationary for 1s for fixation before and after the movement (Fig. 1B). In some neurons (n=4), neuronal responses were tested during pursuit along ± 22.5° of the roughly estimated preferred direction to determine preferred directions more precisely.

To examine the preferred directions for optic flow, the random-dot pattern was moved in 8 cardinal directions while the monkeys fixated a stationary spot in the center of the computer screen. Optic flow stimulation was again given in a ramp trajectory (Fig. 1C). The pattern was first stationary for 1s and then moved at 10°/sec for 2 s. Receptive field mapping of optic flow stimulation was done while the monkeys fixated the central stationary spot. The random-dot pattern was moved along the preferred direction while shifting the center of the pattern by 12° from the center of the display to left, right, top and bottom. Also, a smaller visual pattern (e.g., 5 × 5°) was used to examine roughly the receptive field size and whether the receptive field included the ipsilateral hemifield.

Neuronal responses during smooth-pursuit and optic flow were recorded while upright and during static whole-body roll-tilt, and the preferred directions (re monkeys' head/trunk axis) of task-related neurons were compared. Typically, we tested one tilt position first, followed by upright testing, and finally the other tilt position. In some neurons, we tested upright first, followed by the tilt positions.

To examine whether task-related neurons in MST could signal static roll-tilt, a stationary spot

was presented straight ahead of the monkeys' eyes without a random-dot pattern, and mean discharge rates during fixation were examined while upright and tilted.

Figure 2 near here

Data analysis

Data were analyzed off-line as previously described (e.g. Akao et al. 2005; Kurkin et al. 2007). Neuronal discharge was discriminated with a dual time-amplitude-window discriminator and digitized together with eye position and target position signals at 500 Hz using a 16-bit A/D board. Eye position signals were differentiated to obtain eye velocity. Saccades were removed from eye velocity traces using our interactive computer program (Fukushima et al. 2000). All traces were aligned on stimulus onset using about 10 trials, to allow construction of raster and histograms of neuronal responses.

Neuronal responses were evaluated as the mean discharge rate during analysis interval defined by the latencies of the responses (see Fig. 4). The two vertical lines in Fig. 1B and C illustrate the analysis interval. During smooth-pursuit (Fig. 1B), the analysis interval was defined as the period between 200 ms and 1200 ms after the onset of target motion (Newsome et al. 1988). During optic flow stimulation (Fig. 1C), the mean discharge rate was calculated for a period of 50 – 2050 ms during fixation after the onset of pattern motion. Mean discharge rates in 8 cardinal directions were calculated.

To examine whether neurons responded during smooth-pursuit and/or optokinetic stimuli, mean discharge rate and standard deviation (SD) of the mean rate for the 500-ms interval immediately before target or pattern motion onset were calculated as the control. If the mean discharge rate during the analysis interval exceeded 2SD of the control value in at least one of the eight directions, the neuron was classified as a responding neuron (Table 1: "responded"). If the mean discharge rate did not exceed 2SD of the control rate in all directions, the neuron was classified as not responding (Table 1: "no").

The preferred direction of each neuron was estimated using the Gaussian function:

$$y = A0 + A \times exp\ [-0.5 \times ((x - x0)/s)\ ^2] \qquad (1)$$

where *y* is discharge in direction *x*, *A0* is the resting rate, *A* is the maximal discharge rate at the preferred direction, *x0* is the preferred direction, and *s* characterizes the width of the Gaussian (Colby et al. 1993; Gottlieb et al. 1994; Krauzlis and Lisberger 1996; Kurkin et al. 2007). Mean discharge rates in 8 directions were fit with the Gaussian function (1) using the Levenberg-Marquardt algorithm (Press et al. 1992, Fig. 2A-B). SD of individual data points was calculated using a bootstrap procedure (N=2000) applied during averaging of individual spike traces (e.g., Fig. 2B, left).

To test whether the changes in preferred directions during static roll-tilt were not simply a reflection of the inherent variability of responses of each neuron, we calculated preferred direction and SD of the preferred direction for each neuron by the fitting procedure (e.g., Fig. 2B, right). As an uncertainty level, we used 2SD. For example, the neuron shown in Fig. 2 (A, B) had the preferred direction of 303.5°, and SD was 1.1° (Fig. 2B, right). Therefore, changes smaller than ±2.2° were considered as insignificant for this neuron in this task condition. Mean SD for a total of 293 task conditions in 49 neurons was 5.0° ± 3.4SD° (up to 9 conditions were tested for each neuron). When comparing preferred directions in upright and tilted conditions (either RED or LED, e.g., Fig. 6B), a pooled SD was calculated from two SDs of the corresponding preferred directions.

To examine latencies of neuronal responses to optic flow and spot motion, more than 10 traces were aligned on the onset of target or pattern motion. Traces in which saccades appeared within ~200 ms of the target/pattern onset were omitted. Mean discharge rate and standard deviations (SD) of the mean rate were calculated for the 500-ms interval immediately before target/pattern motion onset, and these values were used as the baseline. Onset of responses to target/pattern motion was determined as the time at which the mean discharge rate exceeded 2 SD of the baseline value (Fig. 2C). Latencies of eye movement responses were measured as the time at which the mean oppositely directed (e.g., upward/downward) eye velocities diverged.

To examine whether task-related neurons in MST could signal static whole-body roll-tilt, mean

discharge rate and the coefficient of variation (CV) of the mean rate were calculated during fixation of a stationary spot straight ahead of the monkeys for 2 s while upright and tilted. The 2-second period was divided into consecutive 100 ms bins and mean discharge rate and SD were calculated. The CV was calculated by dividing the SD by the mean discharge rate in order to examine the variability of discharge rate during fixation.

Histological procedures

Near the conclusion of recordings in monkey S, the recording sites were marked by passing current (50 μA for 30 s) through the tip of a iron-plated tipped, tungsten electrode. After recording was completed, this monkey was deeply anesthetized with pentobarbital sodium (50 mg/kg, i.p.) and perfused with physiological saline followed by 3.5 % formalin. After histological fixation, coronal sections were cut at 100-μm thickness on a freezing microtome. These sections were stained using the Nissl method and the recording sites were verified microscopically as previously described (Akao et al. 2005). Recording sites of monkey Y were confirmed histologically in a similar manner.

Table 1, Figures 3 and 4 near here

Results

We tested the effect of static whole-body roll-tilt using position-ramp trajectories (Fig. 1B, C, see Materials and Methods) in a total of 51 neurons in MST that showed discharge modulation during smooth-pursuit with a stationary background pattern in 2 monkeys (35 from monkey Y, 16 from monkey S). The number of neurons tested varied between tasks due to the occasional degradation or loss of neural recordings.

Classification of MST neurons during smooth-pursuit and optic flow stimulation

We classified the 51 neurons as belonging to one of 4 groups on the basis of their responses to optic flow and smooth-pursuit without a stationary background pattern (Table 1). The majority (35/51, 69 %) of MST neurons tested responded to both optic flow and smooth-pursuit eye movements (Type A). Ten (19 %) neurons responded to smooth-pursuit alone (Type B) and 5 (10 %) neurons responded to optic flow alone (Type C). All of these neurons showed strong directional selectivity

and the neurons that responded to optic flow stimulation had large visual receptive fields, and in many of them, the ipsilateral hemifield was included, similar to the discharge properties of MST neurons in previous studies in this laboratory (Akao et al. 2005). These response properties are typical of neurons in MSTd (Komatsu and Wurtz 1988a).

In Fig. 3, we compare the preferred directions of visual motion and pursuit responses of type A neurons. In the majority (29/35, 83 %) of them, preferred directions of the two responses were oppositely directed (surrounded by solid lines). These neurons were classified as Type A (opposite). In the remaining 6 neurons, the two responses had similar preferred directions (surrounded by dashed line in Fig. 3). They were classified as Type A (same). In 4 type A neurons, 3 had opposite preferred directions and 1 had same preferred directions during smooth-pursuit and optic flow stimulation. Preferred directions of these 4 neurons are not plotted in Fig. 3 because insufficient data were acquired to perform the Gaussian analysis for optic flow responses.

Latencies of neuronal responses to optic flow stimulation (i.e., fixation) and position-ramp spot motion (i.e., pursuit) are illustrated in Fig. 4. In response to optic flow, the median latency was 74 ms and mean latency was 80 ms (Fig. 4A). During smooth-pursuit, the median was 212 ms and mean latency was 242 ms (Fig. 4B). Only 4 neurons (9.3%) discharged before the onset of pursuit eye movements (Fig. 4B: open bars). The remaining neurons tested discharged after the onset of eye movements. The mean latency of smooth-pursuit eye movement to the onset of target motion was 119 ms (Fig. 4B: arrow).

Figures 5 and 6 near here

Comparison of preferred directions when upright and during static whole-body roll-tilt

Figure 5 shows discharge of a representative neuron as the animal pursued a target in the neuron's preferred direction (i.e., rightward) when upright (C) and during static whole-body roll-tilt (A: right ear down RED; E: left ear down LED). This neuron discharged similarly during the three conditions (Fig. 5A, C, E). The preferred direction estimated using a Gaussian fit was 6.4° ±4.3SD when upright (Fig. 5D). If the pursuit signal of this neuron was coded in the earth-centered coordinate, the

expected preferred directions during 40° static roll-tilt would be the same relative to gravity (i.e., rightward) irrespective of the monkey's whole-body roll-tilt. The expected preferred direction of this neuron during 40° RED (6.4 + 40 = 46.4°) and 40° LED (6.4 - 40 = -33.6°) in the earth-centered coordinate are indicated in Fig. 5B and F (gray arrows and lines, respectively). Actual preferred directions (relative to monkey's head/trunk axis) were 12.6°±5.6SD during the RED condition (solid line in Fig. 5B) and 0.0° ±2.7SD during the LED condition (solid line in Fig. 5F), and were clearly different from the directions expected from the earth-centered coordinate (gray arrows and lines in Fig. 5B, F).

To further examine whether the frame of the LCD display influenced the preferred directions of pursuit and/or visual motion signals in MST, responses of 5 neurons were tested while the frame of the display was occluded by an earth-fixed cover. This cover showed only the central portion of the display such that it had the identical orientation relative to earth-centered axis when upright and during static roll-tilt. In all 5 neurons tested, the preferred directions were similar when upright and during tilt positions, indicating that the frame of the display did not influence the preferred directions of these neurons.

Preferred directions of a total of 51 MST neurons tested when upright and during 40° static whole-body roll-tilt are illustrated in Figs. 6, 7 and 8. For almost all neurons tested, preferred directions when upright and during static whole-body roll-tilt (RED and LED) were similar. In the smooth-pursuit only condition, we compared preferred directions between upright and static whole-body roll-tilt in a total of 38 neurons. These neurons include 23 Type A (opposite), 6 Type A (same) and 9 Type B neurons (see Table1). Figure 6A compares, in different colors, the distribution of preferred directions of each type of neurons during upright, RED and LED positions. Figure 6B plots the differences in preferred directions between upright and RED (upper graph) and between upright and LED (lower graph). Gray arrows in Fig. 6B indicate the effect expected from ocular counter-rolling, which is compensatory eye movement observed during static roll-tilt (Collewijn et al. 1985; Leigh and Zee 2006). In previous studies in our laboratory, the gain of ocular counter-rolling during static whole-body roll-tilt in Japanese monkeys was very small (0.09 – 0.13,

Suzuki et al. 1997). The horizontal dashed lines in Fig. 6B indicate the expected range of ocular counter-rolling (i.e., 6°), assuming that the gain of ocular counter-rolling was 0.15. Differences in preferred directions of the majority of neurons were small. Mean ±SD differences in preferred directions of all neurons tested during upright and RED in the counter-clockwise (CCW) and clockwise (CW) directions were -5.0±4.0SD° and 4.7±3.6°, respectively (Fig. 6B, upper graph). Mean ±SD differences in preferred directions of all neurons tested during upright and LED in the clockwise and counter-clockwise directions were 4.5±3.7° and -3.5±1.8°, respectively (Fig. 6B, lower graph). The 3 types of MST neurons (Fig. 6B) exhibited mostly similar distributions. The bars with an asterisk in Fig. 6B indicate neurons (n=6) with the difference larger than 10° (see below).

We also evaluated shifts of preferred directions during static roll-tilt based on the variability of response of individual neurons. The preferred direction and SD of the preferred direction were calculated for each neuron (see Data analysis). Table 2A summarizes number of neurons during smooth-pursuit only condition whose preferred directions were shifted $\geq$ or < 2SD of the preferred directions of each neuron in the counter-clockwise or clockwise directions during RED and LED conditions. The number of neurons whose preferred directions were shifted $\geq$ 2SD in the ocular counter-rolling direction (Fig. 6B, arrows) were slightly larger than those shifted in the opposite direction during the RED condition (upright – RED, n=4 vs 2). However, there was no difference during the LED condition (upright – LED, n= 2 vs 2).

Table 2, Figures 7 and 8 near here

Figure 7A and B summarize the distribution of preferred directions (A) and differences in preferred directions between upright and right/left ear down (B) during optic flow stimuli for a total of 32 neurons. These neurons include 25 Type A (opposite), 2 Type A (same), and 5 Type C. Mean (±SD) differences in preferred directions of all neurons tested during upright and RED in the clockwise (CW) and counter-clockwise directions (CCW) were 4.7±2.7° and -4.6±3.2°, respectively (Fig. 7B, upper graph). Mean (±SD) differences in preferred directions during upright and LED in

the clockwise and counter-clockwise directions were 5.2±4.3° and -5.2±3.7°, respectively (Fig. 7B, lower graph). Differences in preferred directions of individual neurons were distributed mostly similarly towards counter-clockwise and clockwise directions (Fig. 7B).

Table 2B summarizes number of neurons during optic flow only condition whose preferred directions were shifted $\geq$ or < 2SD of the preferred directions of each neuron in the counter-clockwise or clockwise directions during RED and LED conditions (see Data analysis). Only 2 neurons exhibited shifts of preferred directions $\geq$ 2SD. There was no consistency in the shifts of preferred directions towards a particular direction (Table 2B).

Finally, Fig. 8 illustrates the result of smooth-pursuit with a stationary background pattern, which combines smooth-pursuit and optic flow stimulation. In Fig. 8, responses of a total of 44 neurons were examined during static roll-tilt (24 Type A (opposite), 6 Type A (same), 9 Type B, 4 Type C and 1 Type D, see legend for Table 1). With combined pursuit and visual stimuli, preferred directions were mostly similar. Mean (±SD) differences in preferred directions during upright and RED in the clockwise (CW) and counter-clockwise (CCW) directions were 4.9±2.8° and -5.1±3.4°, respectively (Fig. 8B, upper graph). Mean (±SD) differences in preferred directions during upright and LED in the clockwise and counter-clockwise directions were 3.6±2.3° and -3.2±2.1°, respectively (Fig. 8B, lower graph). These results suggest that the shifts of preferred directions of pursuit/visual signals of the majority of MST neurons tested were similar in the clockwise and counter-clockwise directions during static whole-body roll-tilt irrespective of the direction of roll-tilt (Figs. 6B, 7B, 8B).

Table 2C summarizes number of neurons during smooth-pursuit + optic flow condition whose preferred directions were shifted $\geq$ or < 2SD of the preferred directions of each neuron in the counter-clockwise or clockwise directions during RED and LED conditions (see Data analysis). Only a few neurons exhibited shifts of preferred directions $\geq$ 2SD. Shifts of preferred directions occurred both in the ocular counter-rolling direction and opposite direction (Table 2C).

Figure 9 near here

Shifts of preferred directions

To the best of our knowledge, the maximum reported gain of ocular counter-rolling during static roll-tilt in monkeys was 0.24 (Krecjova et al. 1971). This corresponds to 9.6° during 40° static roll-tilt used in our study. For 10 of 51 neurons, the preferred directions were shifted over 10°. These neurons are denoted by an asterisk in Figs. 6, 7, and 8, and include 6 Type A (opposite), 2 Type A (same) and 2 Type B neurons. In the 10 neurons, the maximum shift was 14° and the mean shift was 12°. Although these shifts were larger than the range expected from ocular counter-rolling (i.e., 9.6°), it was much smaller than the expected shift of ~40° if MST signals were coded in the earth-centered coordinates (see Discussion). For the 10 neurons we also tested whether peak discharge rates could code tilt direction. None of them exhibited peak discharge rates associated with the shifts of preferred directions.

Comparison of mean discharge rates when upright and during static whole-body roll-tilt

To examine whether MST neurons could signal static whole-body roll-tilt, we compared mean discharge rate during fixation of a stationary spot for upright and whole-body roll-tilt. Mean discharge rates of the 46 neurons are plotted in Fig. 9A during upright, RED, and LED. Although some neurons exhibited a difference, in the majority of neurons the difference was small. Mean (±SD) discharge rates during upright, RED and LED conditions were 7.9±6.0, 6.1±5.3 and 8.1±6.6 spikes/s, respectively. In Fig. 9A, mean rates are shown by open squares connected by thick lines.

To examine variability of discharge rates during fixation while upright and during static whole-body roll-tilt, we calculated the CV of the mean discharge rate for each neuron (see Materials and Methods). The CVs ranged from 0.51 to 4.47 and were similar for each neuron in each condition. Mean CVs was 1.59. In Fig. 9B, we plotted the difference in discharge rate between upright and roll-tilt conditions for each neuron against the mean discharge rate when upright (diamonds: upright – RED, squares: upright – LED). The absolute differences in discharge rates of individual neurons ranged from 0 to 8.5 spikes/s. The mean differences (±SD) between upright and RED were 0.6 ± 1.9 spikes/s and the mean differences between upright and LED were 0.1 ± 2.6

spikes/s. The oblique dashed lines in Fig. 9B indicate the expected error ranges that were estimated from the minimum CV. Almost all neurons tested were within the error ranges (except for 2 neurons: arrows). Filled diamonds and squares indicate the discharge rate differences of the neurons that showed more than 10° shifts in preferred directions between upright and tilt positions. All filled marks were within the expected error ranges. These results suggest that virtually all neurons tested did not exhibit a significant difference in discharge rate during fixation between upright and whole-body roll-tilt positions.

Figure 10 near here

Recording location

Figure 10 illustrates representative recording tracks in monkey S and Y. Most of the tracks passed through the rostral bank of the superior temporal sulcus. In both monkeys, recording tracks were found within or in close vicinity of MSTd.

Discussion

Pursuit eye velocity and visual motion signals in MSTd during static whole-body roll-tilt

Our results were collected from 51 MSTd neurons and indicate that the preferred directions (re monkeys' head/trunk axis) of pursuit and visual motion responses for the majority of them (41/51=80%) were similar when upright and during 40° static whole-body roll-tilt (Figs. 6A, 7A, 8A). Shifts of preferred directions were small and there was no consistency in the shifts of preferred directions towards a particular direction (Figs. 6B, 7B, 8B, Table 2).

We were unable to discriminate head-centered and eye-centered coordinates because we did not record torsional eye movements. However, if the shift could be accounted for by the expected counter-rolling of the eye during static roll-tilt, we should have observed shifts of preferred directions consistently towards the direction of ocular counter-rolling (e.g., Fig. 6B). However, there was no consistency in preferred directions (Figs. 7B, 8B). This inconsistency was also seen by evaluating the inherent variability of responses of individual neurons (Table 2A-C). Moreover, the small shifts of preferred directions of the minority of neurons were still much smaller than the

expected shift of ~40° if MST signals were coded in the earth-centered coordinate (Fig. 6B, 7B, 8B). Thus, none of 51 MSTd neurons tested does not signal pursuit eye velocity and/or visual motion directions in the earth-centered coordinate. Rather, our results suggest that these signals were coded in the head and/or trunk-centered coordinates.

In the present study, we postulated that, if MSTd is involved in perception of motion direction (e.g., Gu et al. 2007; Liu and Angelaki 2009), the coordinate representing visual motion signals during static roll-tilt would be earth-centered and that MSTd neurons would signal static whole-body roll-tilt, because it has been shown that monkeys can perceive the earth-centered axis as accurately as humans during static roll-tilt and that otolith inputs contribute dominantly to the perception (see Introduction, Kaptein and Van Gisbergen 2004; Dadaoua et al. 2008; Lewis et al. 2008). Our negative results suggest that at least the MSTd neurons we tested are unlikely to be directly involved in perception of visual motion direction. However, unlike the task conditions used by Gu et al. (2007, 2008), our search task did not specifically ask the monkeys for perception of visual motion direction. So, we still cannot exclude the possibility that our search task missed a subset of MSTd neurons that may have been specifically involved in motion direction perception. Another possible reason for our finding that most MST neurons seemed to respond in the head-centered coordinate is the distance between the visual stimuli and the monkeys (i.e., 20.5 cm). Since the visual stimuli were presented within arm's reach and in the animal's personal space, they might be perceived in the head-centered coordinates These possibilities need to be tested in future studies. Also, it should be noted that our results do not preclude the possibility that the perception might be taking place downstream of MSTd.

Recently, Liu and Angelaki (2009) have reported that MSTd neurons respond selectively to heading but not to changes in orientation with respect to gravity. Our results are consistent with their observations (Liu and Angelaki 2009). Ilg et al. (2004) suggested that MSTl neuron discharge during combined eye and head pursuit codes target motion relative to the external world by combining information from retinal motion, pursuit eye velocity, and the head rotation signals. We did not record in MSTl and the possibility remains that MSTl neurons may have earth-centered

coordinates.

It has been shown that neurons in MST, including MSTd, receive otolith inputs induced by horizontal whole-body translation (Duffy 1998; Gu et al. 2007). It has also been shown that MSTd neurons respond to dynamic roll-tilt (Chen et al. 2008). We, therefore, expected that MSTd neurons would also respond to static roll-tilt. Possible explanations for our negative result would be; 1) MSTd neurons may respond to dynamic and static roll-tilt differently; and 2) during static whole-body roll-tilt, sensitivity of MST neurons to linear acceleration would be reduced.

In the present study, we were unable to distinguish whether tested MSTd signals are represented in head centered coordinates or trunk centered coordinates. Visual signals that are represented in trunk coordinates have been reported in lateral intraparietal cortex (LIP, Snyder et al. 1998).

Comparison with previous studies during static roll-tilt

Using unanesthetized, paralyzed cats, Tomko et al. (1981) examined the effects of 45° whole-body tilt on receptive field properties of simple (Hubel and Wiesel 1959, 1962) visual cortical neurons. The receptive field orientation of 73 % of the cells examined remained unaltered relative to the head axis after tilt, whereas in the remaining 27 %, receptive field orientations either over- or undershot the retinal tilt by more than 15° (Tomko et al. 1981; see however, Schwartzkroin 1972 using 30° tilt). In the present study, none of MST neurons tested exhibited shifts of visual motion preferred directions or pursuit preferred directions more than 14° during 40° static roll-tilt (Fig. 6B, 7B, 8B).

Possible explanations for the discrepancy between the cat study (Tomko et al. 1981) and the present monkey results are; 1) tilt-compensated signals of feline visual cortical neurons may not be sent to the dorsal (i.e., parietal) pathway but may be sent to the ventral (i.e., temporal) pathway (Ungerleider and Mishkin 1982), 2) tilt-compensated signals may be found in MSTl (see above), and/or 3) there may be species difference in visual motion responses of visual cortical neurons between cats and monkeys. We were unable to test these possibilities in the present study.

Although we still need to test the possibility that MST contains a subset of neurons that are specifically involved in motion direction perception as discussed above, our results showing that

pursuit and visual motion signals of MSTd neurons were most probably represented in head/trunk centered coordinates suggest that transformation of visual motion signals for earth-centered coordinates during static roll-tilt for the subjective visual vertical (SVV) is most probably performed somewhere else. Potential areas would be MSTl (Ilg et al. 2004), visual posterior sylvian area (VPS) (Guldin and Grüsser 1998; Dicke et al. 2008), ventral intra-parietal cortex (VIP, Colby et al. 1993), parieto-insular vestibular cortex (PIVC, Grüsser et al. 1990), and supplementary eye fields (e.g., Bloomberg et al. 1988; Fukushima et al.2006; Shichinohe et al. 2009). Dicke et al. (2008) reported that percept-related neurons were found more frequently in VPS than in V1 and MT/MST. Single neuron recording in these regions during static roll tilt would be necessary to test these possibilities in future studies.

Notes: We thank Dr. Chris R.S. Kaneko for his valuable comments on the manuscript. This research was supported by Grant-in-Aid for Scientific Research on Priority Areas (System study on higher-order brain functions) (17022001) and (C)(20500351) from MEXT of Japan.

Conflict of interest: None declared.

Correspondence to Kikuro Fukushima, Department of physiology, Hokkaido University School of Medicine, Sapporo, 060-8638 Japan. E mail: kikuro@med.hokudai.ac.jp

References

Akao T, Mustari J, Fukushima J, Kurkin S, Fukushima K. 2005. Discharge characteristics of pursuit neurons in MST during vergence eye movements. J Neurophysiol. 93:2415-2434.

Bloomberg J, Melvill Jones G, Segal B, McFarlane S, Soul J. 1988. Vestibular-contingent voluntary saccades based on cognitive estimates of remembered vestibular information. Adv Oto-Rhinolaryngol. 41:71-75.

Bremmer F, Ilg UJ, Thiele A, Distler C, Hoffmann KP. 1997. Eye position effects in monkey cortex. I. Visual and pursuit-related activity in extrastriate areas MT and MST. J Neurophysiol. 77:944-961.

Bremmer F, Kubischik M, Pekel M, Lappe M, Hoffmann KP. 1999. Linear vestibular self-motion

signals in monkey medial superior temporal area. Ann NY Acad Sci. 871:272-281.

Britten KH, van Wezel RJ. 1998. Electrical microstimulation of cortical area MST biases heading perception in monkeys. Nat Neurosci. 1:59-63.

Britten KH, van Wezel RJ. 2002. Area MST and heading perception in Macaque monkeys. Cereb Cortex. 12:692-701.

Cerebrini S, Newsome WT. 1994. Neuronal and psychophysical sensitivity to motion signals in extrastriate area MST of the macaque monkey. J Neurosci. 14:4109-4124.

Celebrini S, Newsome WT. 1995. Microstimulation of extrastriate area MST influences performance on a direction discrimination task. J Neurophysiol. 73:437-448.

Chen A, Gu Y, Takahashi K, Angelaki DE, Deangelis GC. 2008. Clustering of self-motion selectivity and visual response properties in macaque area MST. J Neurophysiol 100: 2669-2683.

Colby CL, Duhamel L, Goldberg, ME. 1993. Ventral intraparietal area of macaque: anatomic location and visual response properties. J Neurophysiol 69: 902-914.

Collewijn H, Van der Steen J, Ferman L, Jansen TC. 1985. Human ocular counterroll: assessment of static and dynamic properties from electromagnetic scleral search coil recordings. Exp Brain Res. 59:185-196.

Daddaoua N, Dicke PW, Thier P. 2008. The subjective visual vertical in a nonhuman primate. J Vis. 8:1-8.

De Vrijer, Medendorp WP, Van Gisbergen JA. 2008. Shared computational mechanism for tilt compensation accounts for biased verticality percepts in motion and pattern vision. J Neurophysiol. 99:915-930.

Dicke P, Thier P. 1999. The role of cortical area MST in a model of combined smooth eye-head pursuit. Biol Cybern. 80:71-84.

Dicke P, Chakraborty S, Thier P. 2008. Neuronal correlates of perceptual stability during eye movements. Eur J Neurosci. 27:991-1002.

Duffy CJ. 1998. MST neurons respond to optic flow and translational movement. J Neurophysiol.

80:1816-1827.

Dürsteler MR, Wurtz RH, Newsome WT. 1987. Directional pursuit deficits following lesions of the foveal representation within the superior temporal sulcus of the macaque monkey. J Neurophysiol. 57:1262-1287.

Dürsteler MR, Wurtz RH. 1988. Pursuit and optokinetic deficits following chemical lesions of cortical areas MT and MST. J Neurophysiol. 60:940-965.

Fuchs AF, Robinson DA. 1966. A method for measuring horizontal and vertical eye movements chronically in the monkey. J Appl Physiol. 21:1068-1070.

Fujiwara K, Akao T, Kurkin S, Fukushima J, Fukuda S, Fukushima K. 2008. Activity of pursuit-related neurons in MST during static roll-tilt. Neurosci Res (Suppl). 61:s173.

Fukushima J, Akao T, Kurkin S, Kaneko CRS, Fukushima K. 2006. The vestibular-related frontal cortex and its role in smooth-pursuit eye movements and vestibular-pursuit interactions. J Vestibular Res. 16:1-22.

Fukushima K, Sato T, Fukushima J, Shinmei Y, Kaneko CRS. 2000. Activity of smooth pursuit-related neurons in the monkey periarcuate cortex during pursuit and passive whole-body rotation. J Neurophysiol. 83:563-587.

Gottlieb JP, MacAvoy MG, Bruce CJ. 1994. Neural responses related to smooth pursuit eye movements and their correspondence with electrically elicited slow eye movements in the primate frontal eye field. J Neurophysiol 72: 1634-1653.

Graziano MS, Andersen RA, Snowden RJ. 1994. Tuning of MST neurons to spiral motions. J Neurosci. 14:54-67.

Grüsser OJ, Pause M, Schreiter U. 1990. Localization and responses of neurones in the parieto-insular vestibular cortex of awake monkeys (Macaca fascicularis). J Physiol. 430:537-557.

Gu Y, Watkins PV, Angelaki DE, DeAngelis GC. 2006. Visual and nonvisual contributions to three-dimensional heading selectivity in the Medial Superior Temporal area. J Neurosci. 26:73-85.

Gu Y, DeAngelis GC, Angelaki DE. 2007. A functional link between area MSTd and heading perception based on vestibular signals. Nat Neurosci. 10:1038-1047.

Gu Y, Angelaki DE, DeAngelis GC. 2008. Neural correlates of multisensory cue integration in macaque MSTd. Nat Neurosci. 11:1201-1210.

Guldin WO, Grüsser OJ. 1998. Is there a vestibular cortex? Trends Neurosci. 21:254-259.

Heuer HW, Britten KH. 2004. Optic flow signals in extrastriate area MST: comparison of perceptual and neuronal sensitivity. J Neurophysiol. 91:1314-1326.

Hubel DH, Wiesel TN. 1959. Receptive fields of single neurons in the cat's striate cortex. J Physiol (Lond). 148:574-591.

Hubel DH, Wiesel TN. 1962. Receptive field, binocular interaction and functional architecture in the cat's visual cortex. J Physiol (Lond). 160:106-154.

Ilg UJ, Schumann S, Thier P. 2004. Posterior parietal cortex neurons encode target motion in world-centered coordinates. Neuron. 43:145-151.

Inaba N, Shinomoto S, Yamane S, Takemura A, Kawano K. 2007. MST neurons code for visual motion in space independent of pursuit eye movements. J Neurophysiol. 97:3473-3483.

Kaptein RG, Van Gisbergen JA. 2004. Interpretation of a discontinuity in the sense of verticality at large body tilt. J Neurophysiol. 91:2205-2214.

Kasahara S, Akao T, Fukushima J, Kurkin S, Fukushima K. 2006. Further evidence for selective difficulty of upward eye pursuit in juvenile monkeys: Effects of optokinetic stimulation, static roll tilt, and active head movements. Exp Brain Res. 171:306-321.

Kawano K, Sasaki M, Yamashita M. 1984. Response properties of neurons in posterior parietal cortex of monkey during visual-vestibular stimulation. I. Visual tracking neurons. J Neurophysiol. 51:340-351.

Kawano K. 1999. Ocular tracking: behavior and neurophysiology. Curr Opin Neurobiol. 9:467-73.

Komatsu H, Wurtz RH. 1988a. Relation of cortical areas MT and MST to pursuit eye movements. I. Localization and visual properties of neurons. J Neurophysiol. 60:580-603.

Komatsu H, Wurtz RH. 1988b. Relation of cortical areas MT and MST to pursuit eye movements.

III. Interaction with full-field visual stimulation. J Neurophysiol. 60:621-644.

Krauzlis RJ, Lisberger SG. 1996. Directional organization of eye movement and visual signals in the floccular lobe of the monkey cerebellum. Exp Brain Res. 109:289-302.

Krejcova H, Highstein S, Cohen B. 1971. Labyrinthine and extra-labyrinthine effects on ocular counter-rolling. Acta Otolaryngol. 72:165-171.

Kurkin S, Akao T, Fukushima J, Fukushima K. 2007. Activity of pursuit neurons in the caudal part of the frontal eye fields during static roll-tilt. Exp Brain Res. 176:658-664.

Leigh RJ, Zee DS. 2006. The neurology of eye movements, 4th ed. New York, Oxford University Press.

Lewis RF, Haburcakova C, Merfeld DM. 2008. Roll tilt psychophysics in rhesus monkeys during vestibular and visual stimulation. J Neurophysiol. 100:140-153.

Lisberger SG, Morris EJ, Tychsen L. 1987. Visual motion processing and sensory-motor integration for smooth pursuit eye movements. Annu Rev Neurosci. 10:97-129.

Liu S, Angelaki DE. 2009. Vestibular signals in macaque extrastriate visual cortex are functionally appropriate for heading perception. J Neurosci. 29:8936-8945.

Newsome WT, Wurtz RH, Komatsu H. 1988. Relation of cortical areas MT and MST to pursuit eye movements. Ⅱ. Differentiation of retinal from extraretinal inputs. J Neurophysiol. 60:604-620.

Page WK, Duffy CJ. 2003. Heading representation in MST: Sensory interactions and population encoding. J Neurophysiol. 89:1994-2013.

Press WH, Teukolsky SA, Vettering WT and Flannery BP. 1992. Numerical Recipes in C (2nd ed.), Cambridge, UK, Cambridge Univ Press.

Saito H, Yukie M, Tanaka K, Hikosaka K, Fukuda Y, Iwai E. 1986. Integration of direction signals of image motion in the superior temporal sulcus of the macaque monkey. J Neurosci. 6:145-157.

Sakata H, Shibutani H, Kawano K. 1983. Functional properties of visual tracking neurons in posterior parietal association cortex of the monkey. J Neurophysiol. 49:1364-1380.

Shichinohe N, Akao T, Kurkin S, Fukushima J, Kaneko CRS, Fukushima K. 2009. Memory and

decision-making in the frontal cortex during visual motion-processing for smooth pursuit eye movements. Neuron. 62:717-732.

Schwarzkroin PA. 1972. The effect of body tilt on the directionality of units in cat visual cortex. Exp Neurol. 36:498-506.

Shenoy KV, Bradley DC, Andersen RA. 1999. Influence of gaze rotation on the visual response of primate MSTd neurons. J Neurophysiol. 81:2764-2786.

Snyder LH, Grieve KL, Brotchie P, Andersen RA. 1998. Separate body- and world-referenced representations of visual space in parietal cortex. Nature. 394:887-891.

Suzuki Y, Kase M, Kato H, Fukushima K. 1997. Stability of ocular counterrolling and Listings plane during static roll tilts. Invest Ophthalmol Visual Sci. 38:2103-2111.

Thier P, Erickson RG. 1992. Responses of visual-tracking neurons from cortical area MST-l to visual, eye and head motion. Eur J Neurosci. 4:539-553.

Tomko DL, Barbaro NM, Ali FN. 1981. Effect of body tilt on receptive field orientation of simple visual cortical neurons in unanesthetized cats. Exp Brain Res. 43:309-314.

Ungerleider LG, Mishkin M. 1982. Two cortical visual systems. In: Analysis of visual behavior. Ingle DJ, Goodale MA, Mansfield RJ, eds. Cambridge (MA): MIT Press. 549–586.

Legends for Tables and Figures

Table 1. Classification of MST neurons. A total of 51 task-related neurons were classified into 4 groups. Type A neurons responded to both smooth-pursuit and optic flow. Type B responded to smooth-pursuit only. Type C responded to optic flow only. One neuron (type D) showed no distinct discharge modulation during optic flow stimulation and smooth-pursuit eye movement despite that it clearly responded to search stimuli (i.e., smooth-pursuit with a stationary background pattern).

Table 2. Variability of responses of individual neurons. Numbers of neurons are shown for each task condition (A-C) whose preferred directions were shifted $\geq$ or < 2SD of the preferred directions of individual neurons. See text for further explanation.

Figure 1. Behavioral tasks used to differentiate head-centered coordinates and earth-centered coordinates and analysis intervals for smooth-pursuit and optic flow. A: A target spot (0.5° in diameter) and/or a random dot pattern were presented on a 15-inch LCD display in an otherwise dark enclosure. The LCD display and the primate chair together with the monkey were tilted in the roll plane to 40° from the earth-centered (either right ear down, RED, or left ear down, LED). B: pursuit. C: optic flow. Analysis intervals were defined by the latencies of responses during pursuit and optic flow (see Fig. 4). Mean discharge rate during the interval was calculated in each direction. The 6 traces in B are horizontal (H) and vertical (V) target position, horizontal and vertical eye position, and the raster and histogram of neuron discharge. The 4 traces in C are horizontal pattern position, horizontal eye position, raster and histogram of neuron discharge. Upward arrows in B and C indicate pattern/target motion onsets. Two vertical lines in B and C demarcate analysis intervals (B: 200-1200ms, C: 50-2050ms).

Figure 2. The method for calculating preferred directions smooth pursuit and latencies of discharge modulation. A: histograms of example neuron discharge during along eight directions. B: Gaussian fit. Dots indicate mean discharge rate in each direction fitted by Gaussian curve from equation (1). The preferred direction was estimated to be 303.5° ±1.1SD$^{\circ}$ for this neuron. C: latencies of discharge modulation (1 bin = 6 ms). Gray arrow indicates the time at which the mean discharge rate exceeded 2 SD of the mean discharge rate calculated for the 500-ms interval immediately before target motion onset. Vertical dashed line and horizontal solid line show target motion onset and 2 SD of the mean responses of baseline period, respectively. A–C are responses from the same neuron.

Figure 3. Comparison of preferred directions during smooth-pursuit and optic flow responses of Type A neurons. Preferred direction of pursuit response of each neuron is plotted against that of visual motion response. Neurons surrounded by solid lines showed opposite preferred directions. Neurons surrounded by dashed line showed similar preferred directions.

Figure 4. Latencies of neuronal responses to optic flow stimulation during fixation (A) and spot

motion during smooth-pursuit (B). Open bars in B indicate neurons that discharged before the onset of smooth-pursuit eye movements. Upward arrow in B indicates mean latency of smooth-pursuit eye movements.

Figure 5. Discharge and preferred direction of a representative neuron while upright or during static roll-tilt. A, B: 40° static roll-tilt towards right ear down (RED) direction. C, D: upright. E, F: 40° static roll-tilt toward left ear down (LED) direction. The four traces in A, C and E are horizontal target position, superimposed horizontal eye position and raster and histograms of neuron discharge. B, D, F (top) illustrate LCD monitor and target motion directions from the monkey's point of view for the three different task conditions. Actual preferred directions are indicated by thick black arrows. Expected preferred directions for earth-centered coordinates are indicated by gray arrows in B and F. B, D, F (bottom) illustrate directional tuning and Gaussian fits for actual responses for each condition. Black and gray lines are actual and expected preferred directions during static roll-tilts, respectively. Dots indicate actual mean discharge rates.

Figure 6. Preferred directions in upright and tilt positions during the smooth-pursuit only condition. A: Distribution of preferred directions of each type of neurons during upright, RED and LED is summarized in different colors. Preferred directions of individual neurons are connected by lines. Open squares with an asterisk indicate neurons whose preferred directions were shifted more than 10°. B: Differences in preferred directions between upright and RED (top) and between upright and LED (bottom). Mean absolute differences between upright and RED were 4.9°±3.8 SD° (range, 0.1°-13.2°) and between upright and LED were 4.0°±2.8 SD° (range, 0.2°-14.1°). Gray arrows and dashed lines indicate the direction and the expected ranges of ocular counter-rolling, respectively. Asterisks indicate neurons with mean absolute differences between upright and tilted positions larger than 10°. CW and CCW indicate clockwise and counterclockwise, respectively.

Figure 7. Preferred directions in upright and tilted positions during optic flow stimulation. The format is the same as in Fig. 6. For further explanation, see text.

Figure 8. Preferred directions in upright and tilted positions during smooth-pursuit with stationary background pattern. The format is the same as in Fig. 6.

Figure 9. Mean discharge rates during fixation of a stationary spot straight ahead of the monkeys' eyes. A: mean discharge rates while upright and during 40° RED or LED. Filled squares indicate discharge rates of individual neurons in each condition. Individual neurons are connected by lines. Open squares connected by thick lines indicates the overall mean discharge rates for all neurons tested in each condition. B: plots discharge rate differences between upright and RED (diamonds) and between upright and LED (squares) against mean discharge rate of each neuron during upright during fixation. Oblique dashed lines indicate the expected error ranges that were estimated from the minimum CV. Almost all discharge rate differences were within the ranges expected from CV (except for 2 cells: arrows). Filled diamonds and squares indicate discharge rate differences of the neurons that showed more than 10° shifts in preferred direction between upright and tilt positions.

Figure 10. Recording sites in monkey S (left hemisphere) and Y (right hemisphere). Representative coronal sections at Posterior 0 in monkey S and Posterior 1 in monkey Y are shown. IPS and STS indicate intraparietal sulcus and superior temporal sulcus.

Table 1

	smooth-pursuit (background -)	optic flow
Type A: 35 (69%)	responded	responded
Type B: 10 (19%)	responded	no
Type C: 5 (10%)	no	responded
Type D: 1 (2%)	no	no

Table 2

		Counter-clockwise		Clockwise		total
		≥2SD	<2SD	≥2SD	<2SD	
A. Smooth-pursuit only	Upright-RED	4	11	2	9	26
	Upright-LED	2	11	2	12	27
B. Optic flow only	Upright-RED	0	10	2	8	20
	Upright-LED	2	14	2	4	22
C. Smooth-pursuit + Optic flow	Upright-RED	3	13	4	9	29
	Upright-LED	2	16	2	11	31
D. TOTAL		13	75	14	53	155

Fig. 1

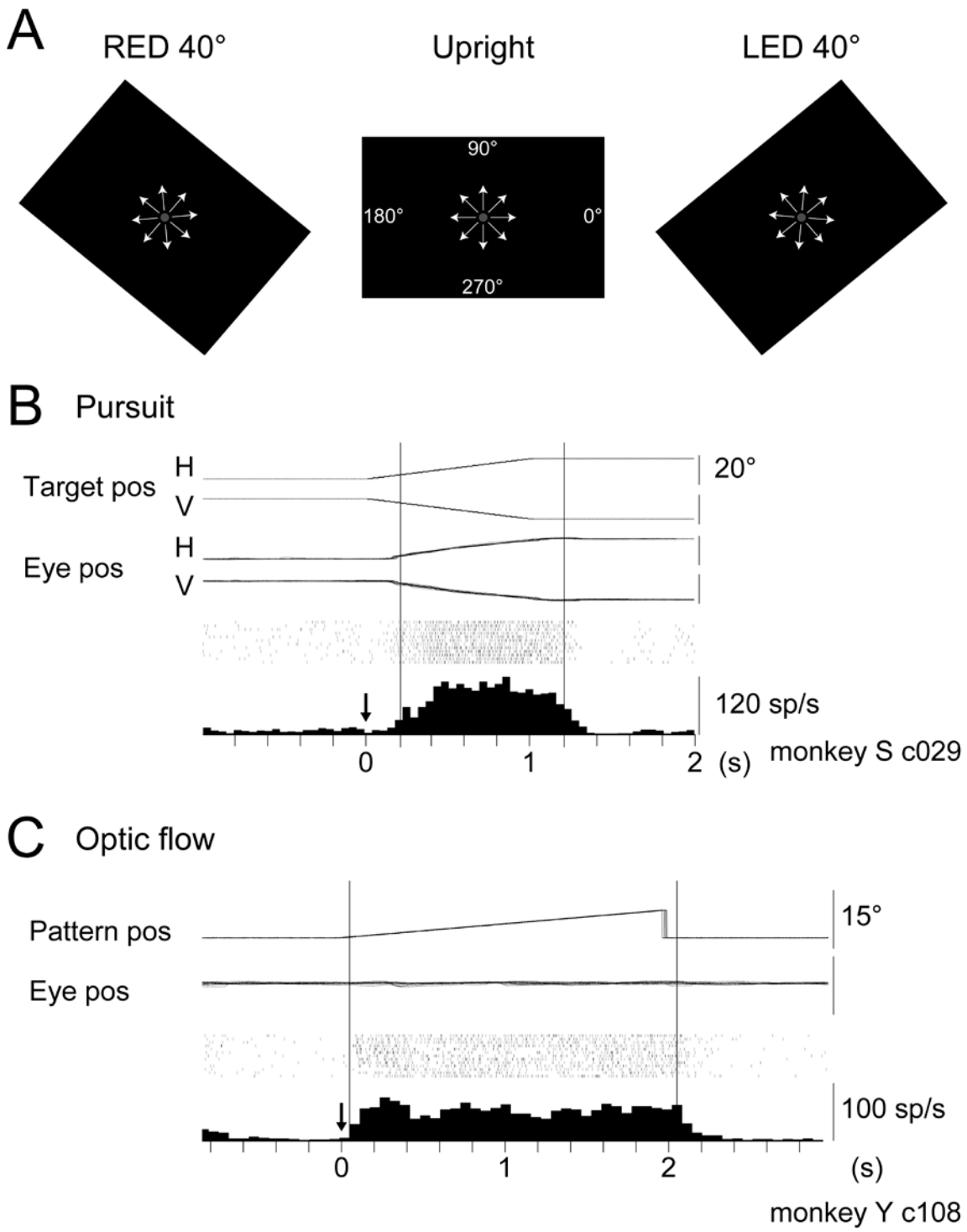
A
RED 40°
Upright
LED 40°
90°
180°
0°
270°
B
Pursuit
Target pos
H
V
Eye pos
H
V
20°
120 sp/s
0
1
2
(s)
monkey S c029
C
Optic flow
Pattern pos
Eye pos
15°
100 sp/s
0
1
2
(s)
monkey Y c108

Fig. 2

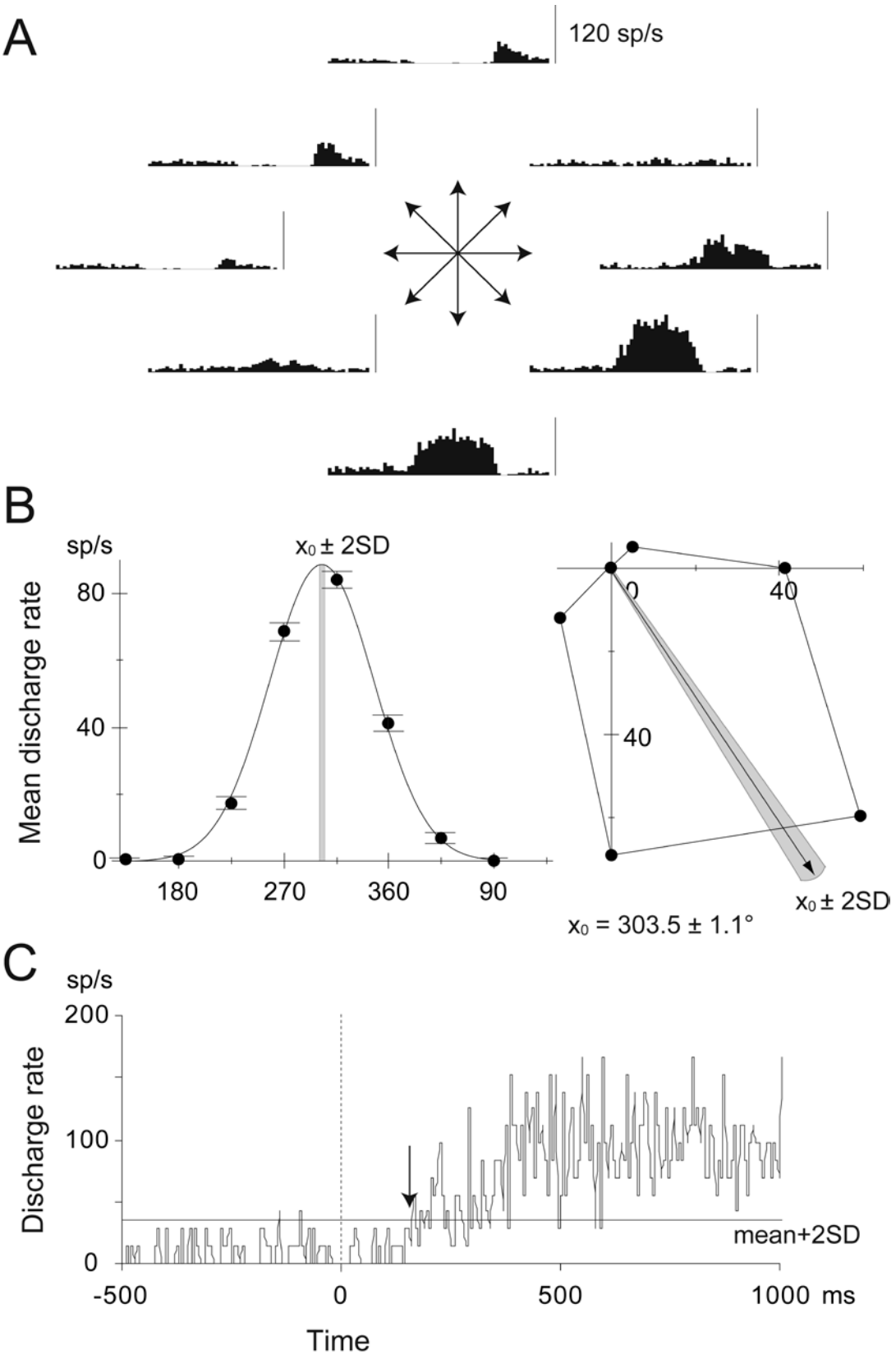
A
120 sp/s
B
sp/s
x0 ± 2SD
Mean discharge rate
80
40
0
180
270
360
90
0
40
40
x0 ± 2SD
x0 = 303.5 ± 1.1°
C
sp/s
200
100
0
Discharge rate
mean+2SD
-500
0
500
1000 ms
Time

Fig. 3

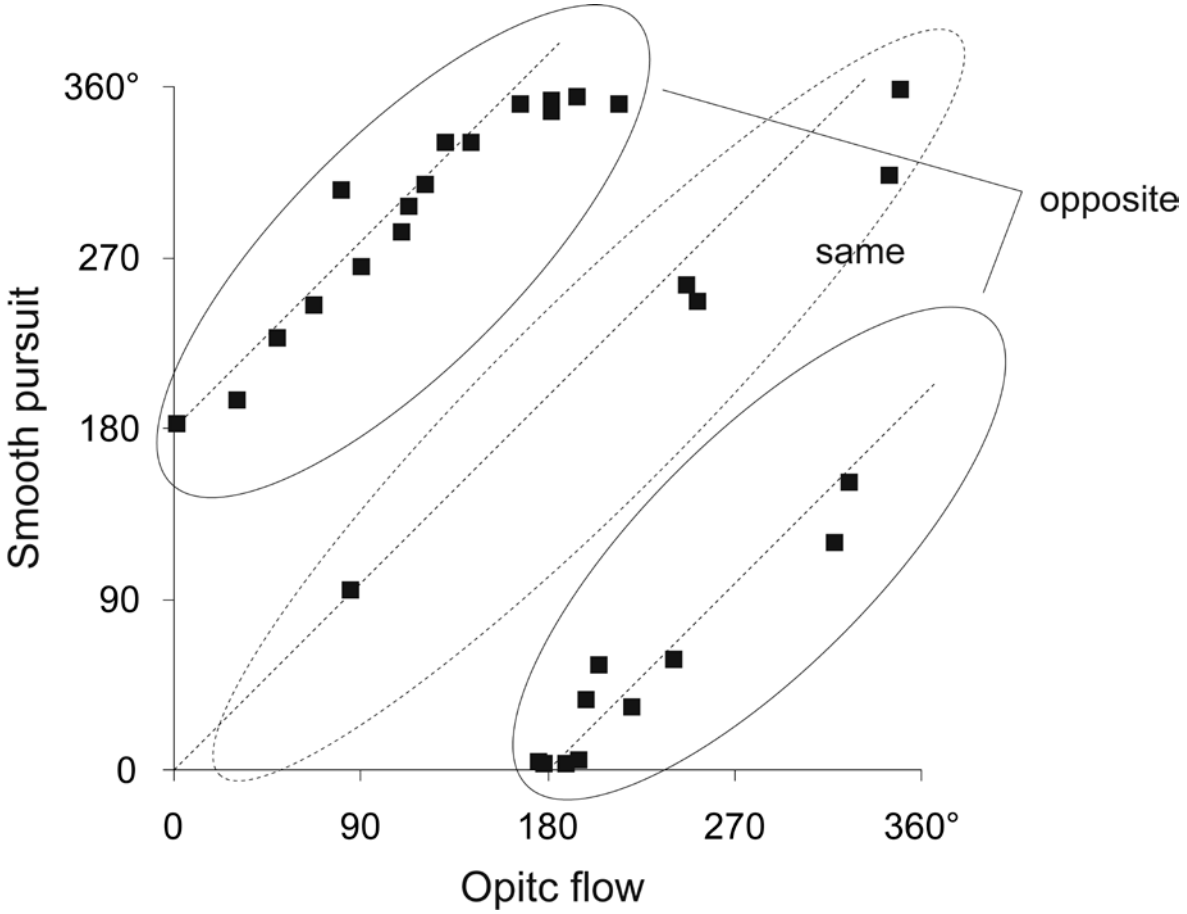
360°
270
180
90
0
Smooth pursuit
0
90
180
270
360°
Opitc flow
same
opposite

Fig. 4

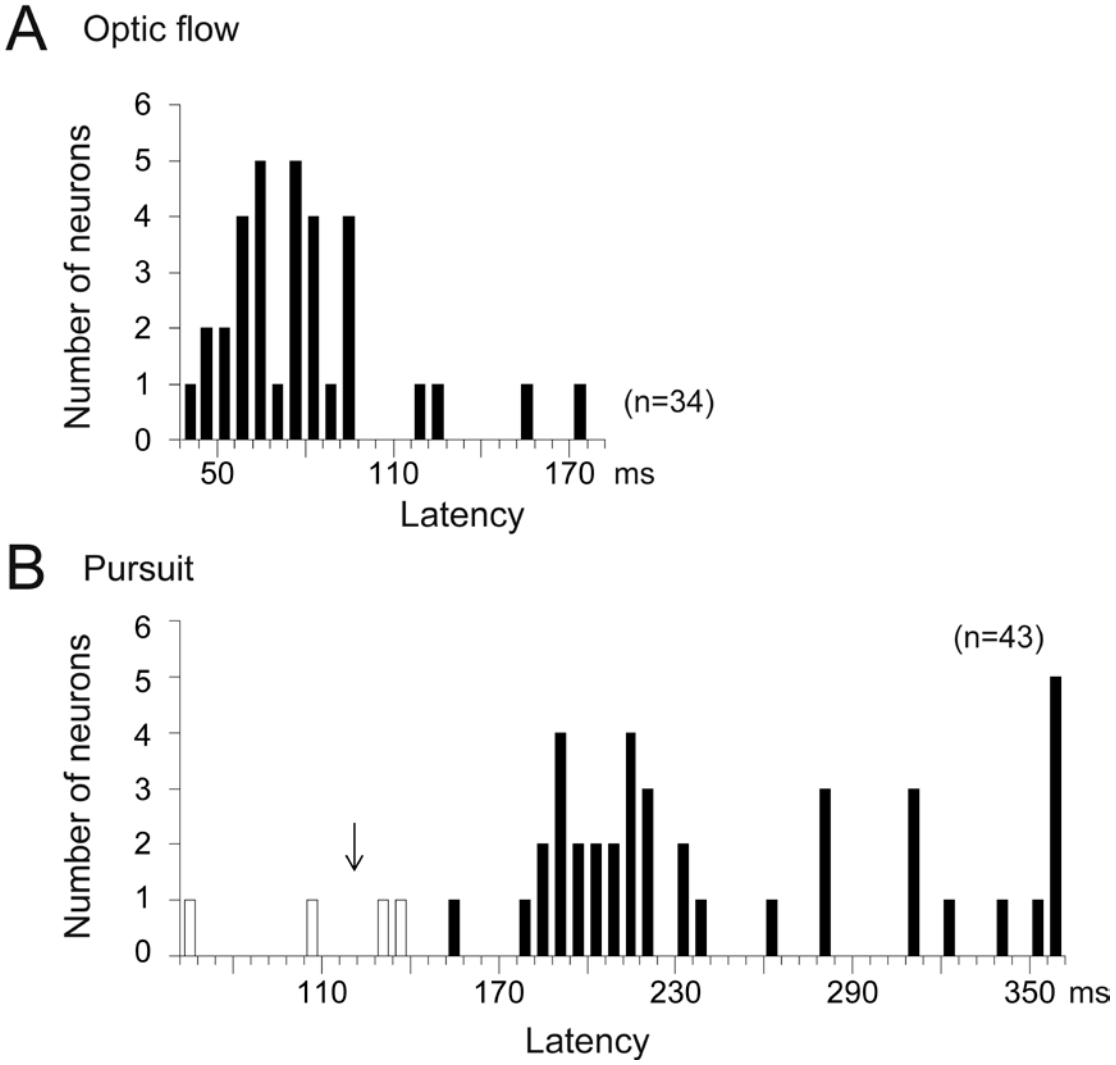
A
Optic flow
Number of neurons
6
5
4
3
2
1
0
(n=34)
50
110
170
ms
Latency
B
Pursuit
Number of neurons
6
5
4
3
2
1
0
(n=43)
110
170
230
290
350
ms
Latency

Fig. 5

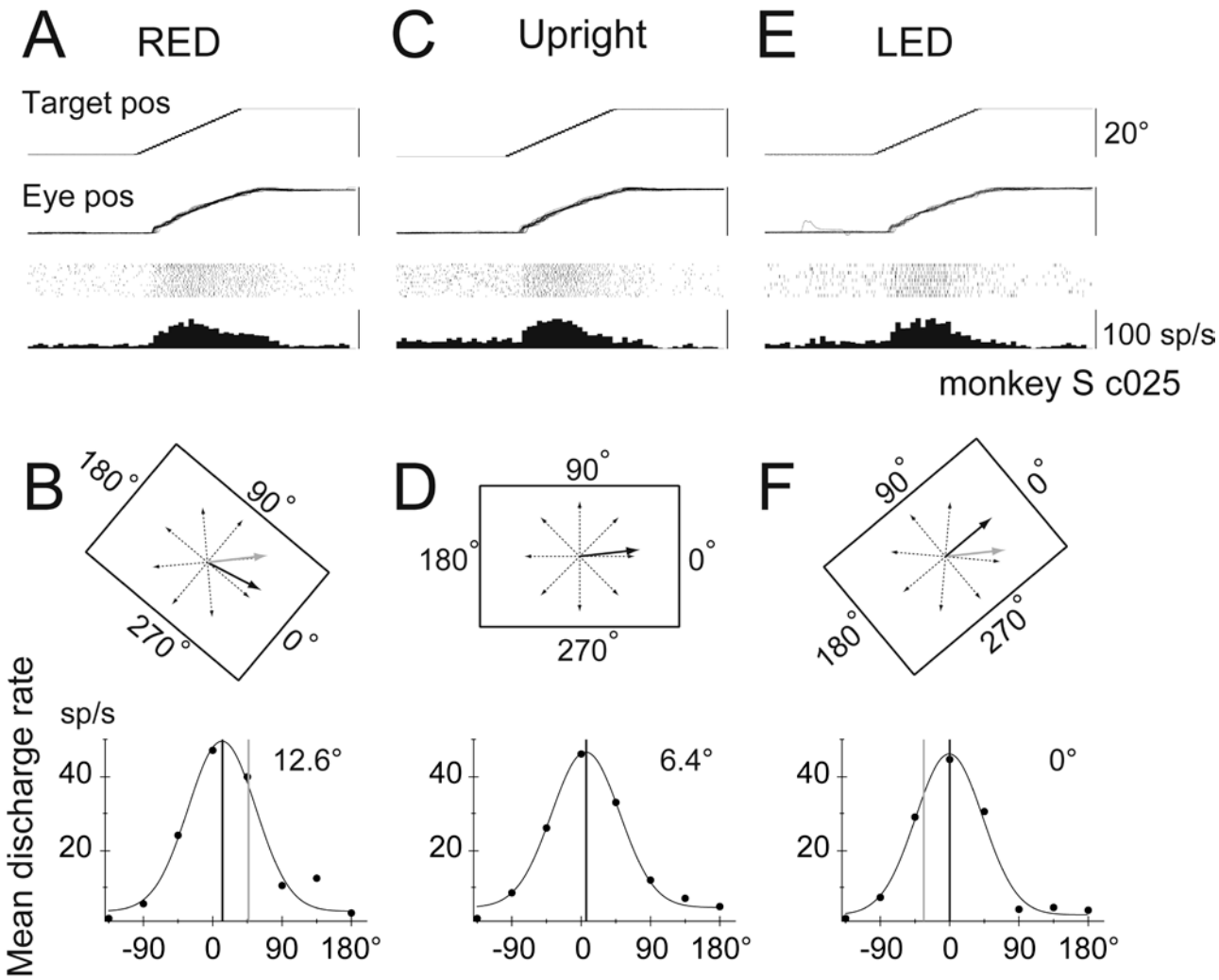
A
RED
C
Upright
E
LED
Target pos
Eye pos
20°
100 sp/s
monkey S c025
B
D
F
180°
90°
0°
270°
Mean discharge rate
sp/s
40
20
12.6°
6.4°
0°
-90
0
90
180°

Fig. 6

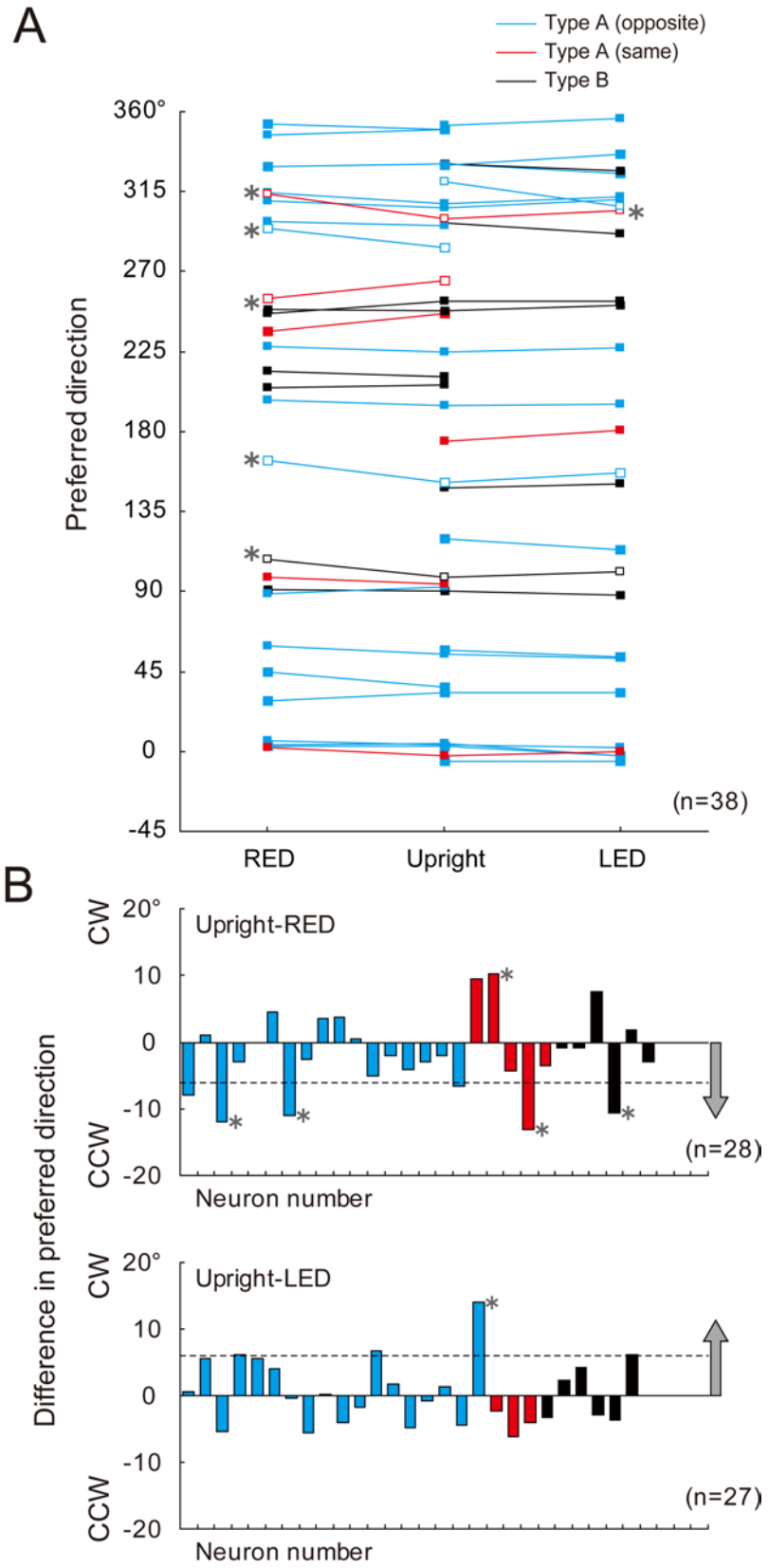
A
Type A (opposite)
Type A (same)
Type B
Preferred direction
360°
315
270
225
180
135
90
45
0
-45
(n=38)
RED
Upright
LED
B
Difference in preferred direction
CW
CCW
20°
10
0
-10
-20
Upright-RED
(n=28)
Neuron number
Upright-LED
(n=27)
Neuron number

Fig. 7

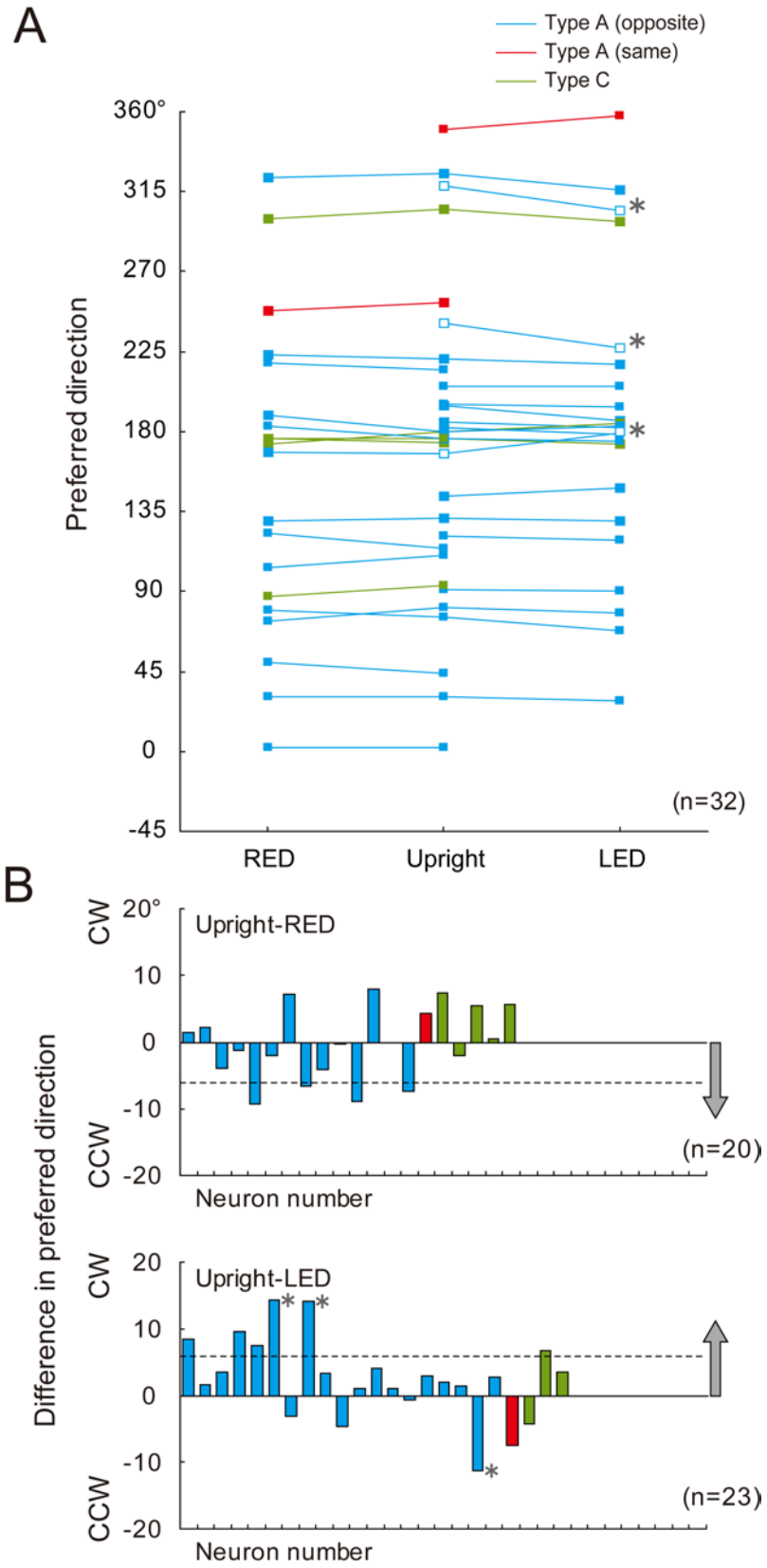
A
Type A (opposite)
Type A (same)
Type C
360°
315
270
225
180
135
90
45
0
-45
Preferred direction
(n=32)
RED
Upright
LED
B
Upright-RED
20°
10
0
-10
-20
CW
CCW
(n=20)
Neuron number
Upright-LED
20
10
0
-10
-20
CW
CCW
(n=23)
Neuron number
Difference in preferred direction

Fig. 8

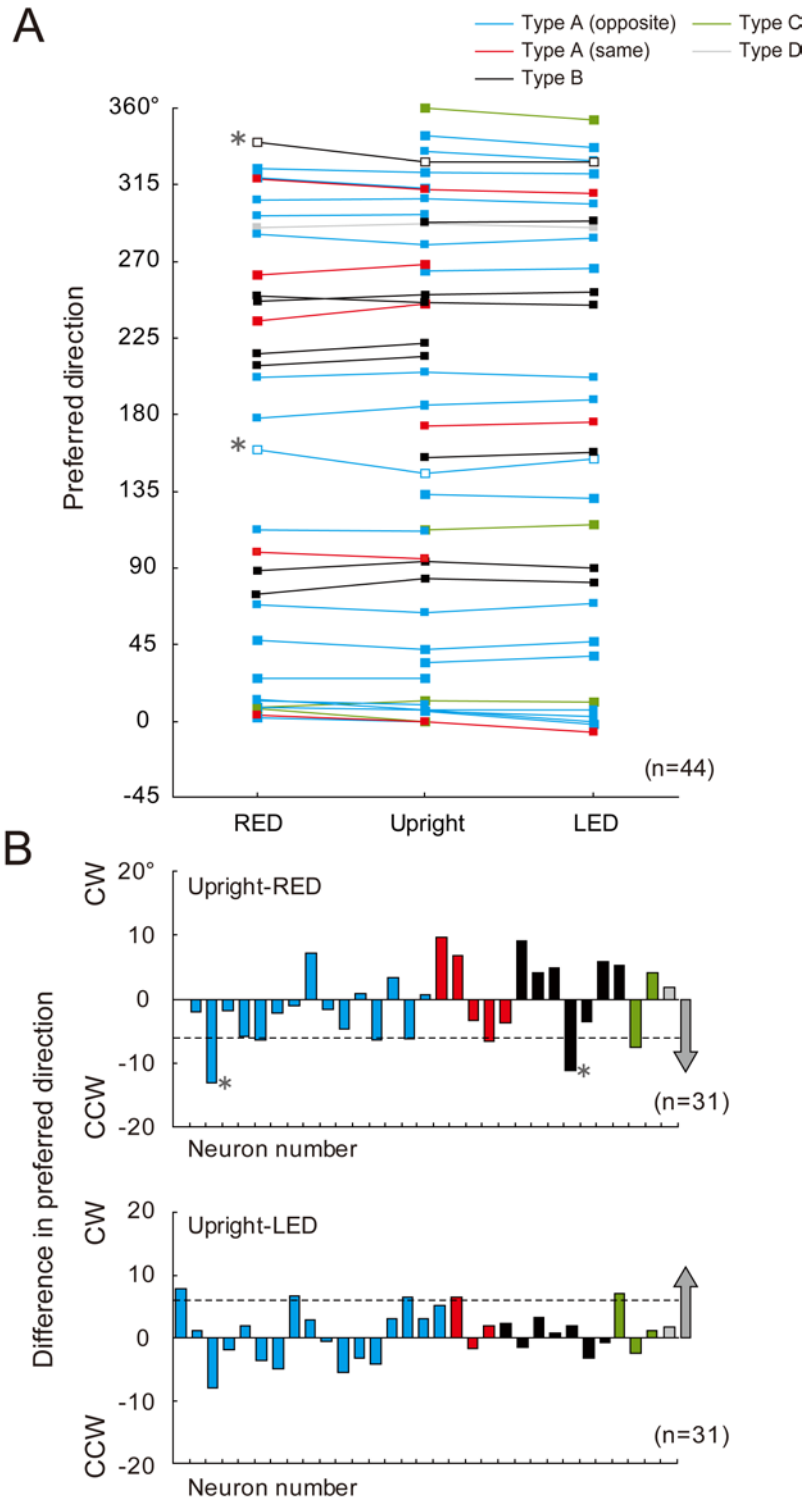
A
Type A (opposite)
Type A (same)
Type B
Type C
Type D
Preferred direction
360°
315
270
225
180
135
90
45
0
-45
(n=44)
RED
Upright
LED
B
Difference in preferred direction
CW
CCW
20°
10
0
-10
-20
Upright-RED
(n=31)
Neuron number
Upright-LED
20
10
0
-10
-20
(n=31)
Neuron number

Fig. 9

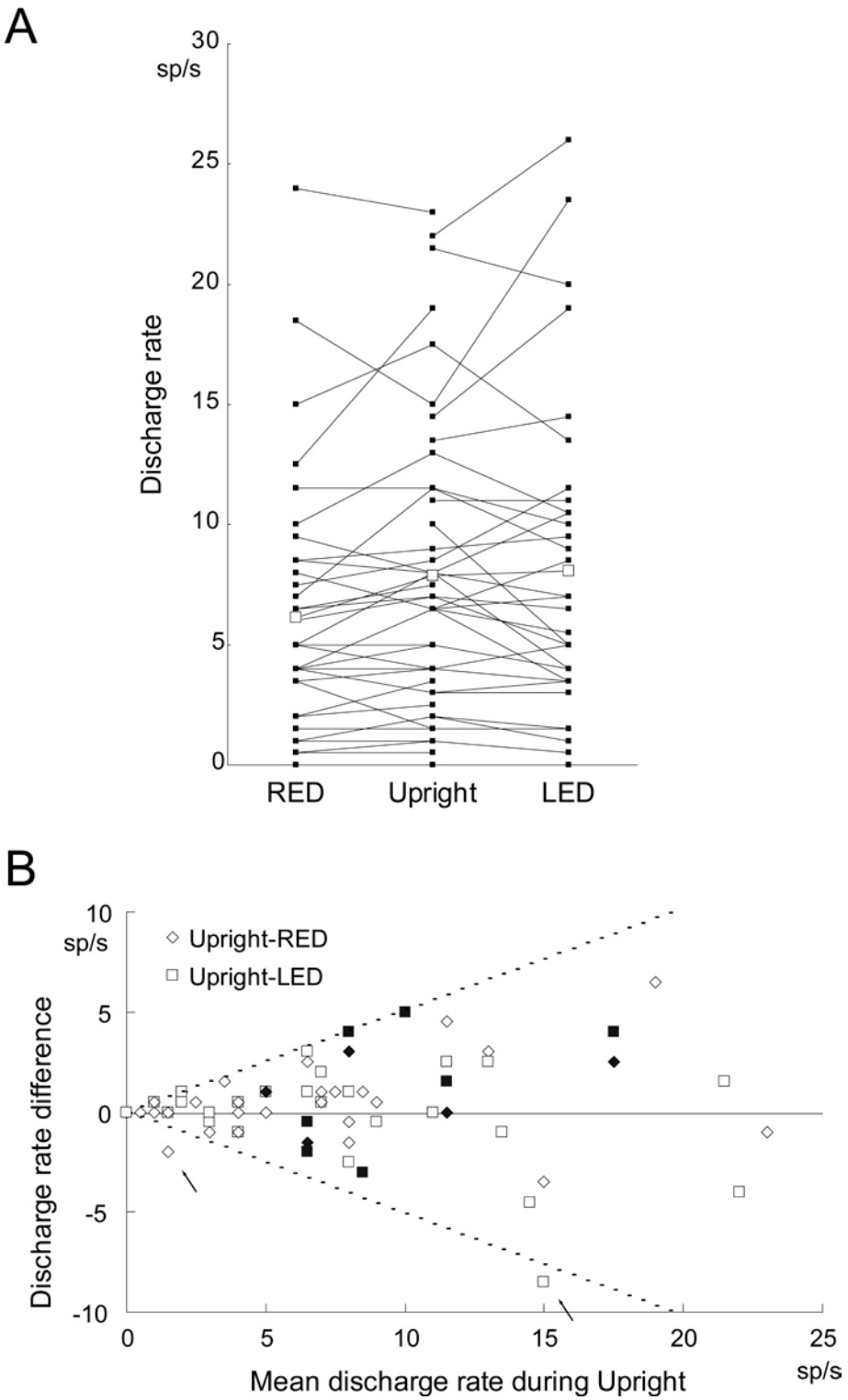
A
30
sp/s
25
20
15
10
5
0
Discharge rate
RED
Upright
LED
B
10
sp/s
Upright-RED
Upright-LED
5
0
-5
-10
Discharge rate difference
0
5
10
15
20
25
sp/s
Mean discharge rate during Upright

Fig. 10

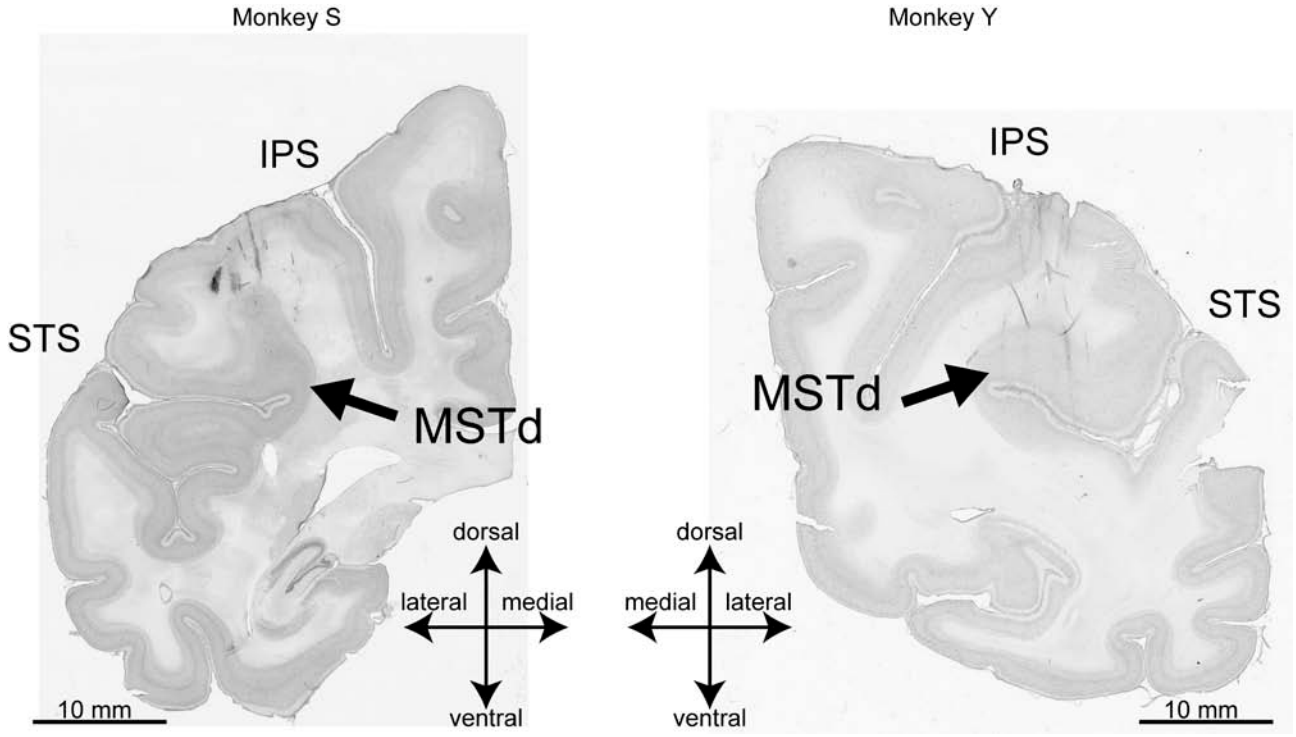
Monkey S
IPS
STS
MSTd
dorsal
lateral
medial
ventral
10 mm
Monkey Y
IPS
STS
MSTd
dorsal
medial
lateral
ventral
10 mm